At-home multispectral imager for the monitoring of blood oxygenation in people at risk of diabetic foot ulcers

Keely Shand[a], Jamie Thomson [b], Sam Philip [c], Jan Boers [d], Craig Robertson[a], Mario Ettore Giardini[a]
[a] University of Strathclyde, United Kingdom; [b] IDCP Scotland Ltd., United Kingdom; [c] JJR MacLeod Ctr. For Diabetes, Endocrinology & Metabolism, NHS Grampian Diabetes Ctr., United Kingdom; [d] RetinaScope BV, Netherlands

ABSTRACT

One in three people living with diabetes are affected by diabetic foot ulcers (DFUs) which, if left unmonitored and untreated, reduce quality of life, and may lead to foot amputation. Regular foot screening is suggested by relevant national guidelines. Yet, compliance with screening is poor, mostly due to the inconvenience of the screening process itself.
In this work, we describe a preliminary version of a simple low-cost device intended for self-monitoring of foot circulation, to identify the areas of poor perfusion expected to be at the root of the formation of DFUs. This device is based on multispectral imaging of the feet in the visible and near-infrared ranges. The device is tested on the hands and feet of a single subject, where impairment of circulation has been simulated through a brief ligature of a finger/two toes. Multispectral images are captured, and a simple machine-learning-based classifier correctly identifies areas of low perfusion on the hand and shows promising data on toes. Albeit the device and the classifier are still susceptible of significant improvement, this is indicative of the fact that the multispectral images contain relevant information on tissue perfusion.

Keywords: Multispectral Imaging, Diabetic Foot, Screening, Perfusion, Diabetes

1. INTRODUCTION

422 million people globally live with diabetes[1] and up to one in three of these people will be affected by diabetic foot ulcers (DFU) in their lifetime [2] . This complication is caused by peripheral neuropathy and vascular abnormalities within the feet that is driven by hyperglycaemia. The combination of these two conditions, if left unmonitored and untreated, can cause a minor injury on the foot to become an ulcer that causes irreversible damage[3]. DFUs reduce quality of life [4], and half of those with ulcers develop fast-spreading infections and complications that require amputation[2].

To prevent ulceration, people living with diabetes are asked to check their feet every day and to attend regular foot screening set out by relevant national guidelines[5]. This screening involves a trained operator performing an assessment of the dermatological, vascular, neurological and musculoskeletal condition of the feet[6], reducing the risk of amputation[7]. Patient compliance to the screening has been shown to affect the recurrence rate of DFU[8]. However, due to screening inconvenience both for patients and for healthcare providers, compliance with DFU screening is poor[9,10].

Current research is trying to make the screening more convenient to patients by developing devices that will aid in at-home monitoring of DFU. Some of the devices currently available monitor indicators of ulcer development, such as inflammation[11–13] or they monitor peripheral neuropathy[14]. Although there has been research into different methods on how to monitor the vasculature of the foot such as near-infrared spectroscopy (NIRS), hyperspectral imaging and transcutaneous oximetry approaches[15], the devices developed still require a trained operator and are therefore not suitable for at-home monitoring.

In this paper, an at-home monitoring device that aims to monitor indicators of blood-oxygen perfusion anomalies without the need for a trained operator is described. Preliminary measurements on a healthy subject's hand and foot are presented.

2. METHODS

The device is a low-cost implementation of a multispectral imager (MSI) that uses visible and infrared reflectance to monitor the blood-oxygen perfusion of the feet. This technique, which has shown potential to monitor DFUs[16,17] was

Clinical Biophotonics III, edited by Daniel S. Elson, Sylvain Gioux, Brian W. Pogue,
Proc. of SPIE Vol. 13009, 1300905 · © 2024 SPIE
0277-786X · doi: 10.1117/12.3017173

chosen as it is non-invasive[15] . With the present work, we are aiming towards implementing it with a format and cost compatible with deployment directly in the home of people living with diabetes and at risk of DFUs.

1.1 The hardware

This at-home MSI comprises of a camera unit and a footrest as seen in Figure 1. The camera unit is a Raspberry Pi Camera Module 2 NoIR (Raspberry Pi Foundation, United Kingdom) in the centre of an illumination ring. The ring contains twenty-four LEDs of five different central wavelengths; 525 nm (Green) (599 Series Single Color, Dialight), 633nm (Red) (599 Series Single Color, Dialight), 740 nm (OIS-150, OSA Opto Light), 770 nm (OIS-150, OSA Opto Light), and 850 nm (WL-SICW Chip LED Infrared Waterclear, Würth Elektronik) plus white LEDs (SM1206UWC, Bivar).The LEDs are placed in a symmetrical configuration within the ring as seen in Figure 2. Both the camera and illumination ring are powered and controlled through a Raspberry Pi 4 (Raspberry Pi Foundation, United Kingdom). This is currently attached to a monitor, mouse and keyboard and designed for future operation via Bluetooth (e.g., via a mobile phone), and a Python (Python Software Foundation, Netherlands) script that switches the LEDs on in sequence and takes the related images. These components are encased in a specifically designed 3D printed encasement. The capture resolution is 640x480 pixels, and the exposure time was set to obtain a number of saturated pixels on the order of 0.01% of the total number of pixels.

To allow the foot sole to be captured, a footrest with a capture window was built from medium-density fibreboard. The footrest had a 177 mm elevation and had an incline of 30˚. The top was then laminated with an anti-reflective clear acrylic panel to act as the pane for the window. For hygiene reasons, the footrest was painted with a gloss paint which allowed it to be wipeable. The internal was painted in Black 3.0 acrylic paint (Culture Hustle – Stuart Semple Store, United Kingdom) to remove reflections. The camera unit was anchored to the base of the footrest on a mount that tilts the camera by 35˚, this was to offset any direct reflections caused by the LEDs during image capture.

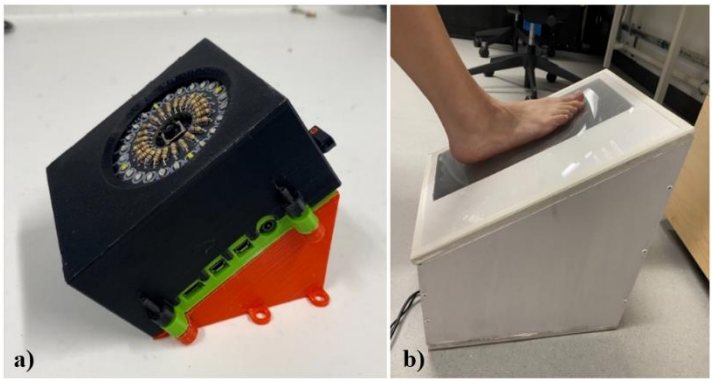

Figure 1. The at-home MSI. A: The camera unit containing the Pi Camera module 2 NoIR, the illumination ring and Raspberry Pi 4. B: The footrest in use, with the subject's foot placed on top of the window.

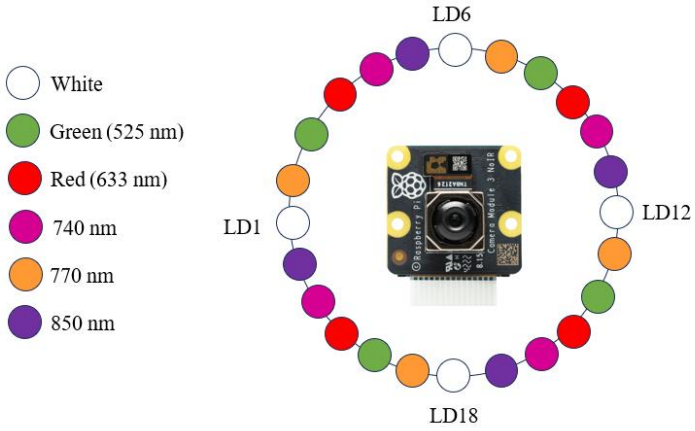

Figure 2. A map of the wavelengths selected for the MSI. There are 5 wavelengths: 525 nm (Green), 633 nm (Red), and Near-Infrared (740 nm, 770 nm, and 850 nm). White LEDs were also added to the ring illumination. These wavelengths are distributed symmetrically throughout the ring.

1.2 Data collection

Images were captured on a healthy subject (one of the investigators) where the subject would first take images without any disruption to blood flow, then occlude blood flow to ring finger (hand), and second and third toe (foot) through a 2-minute temporary ligature, and then re-capturing a set of images. Six un-occluded and five occluded images of the right hand and of the right foot were captured in total, placing the hand/foot over the window on the footrest, and using the device to take six images in rapid sequence.

1.3 Data analysis

One of the hand images and one of the foot images with occluded circulation, randomly chosen amongst the five captured, were used to train a simple pixel classifier. In particular, for each image, the red, green, and blue channel values were extracted as, even in the presence of monochromatic illumination, these carry different spectral information[18], albeit details of the spectral profiles are difficult to determine at this stage, as we do not know the spectral sensitivity of each camera pixel. Additionally, the average intensity of each channel for all illumination wavelengths was calculated and, from this, normalised channel values were calculated.

The hand and the foot images were manually segmented to assign pixels to a region with good blood flow, or to a region with occluded flow, or to the background. Areas not to be used for training to avoid unnecessary unbalancing of the size of the training dataset were also identified.

Simple classification code was written in C# (dotNET Core 8, Microsoft Inc., USA) using Microsoft Visual Studio 2022 (Microsoft Inc, U.S.A.). The ML.NET library[19] was used, utilising the AutoML functionality, which identified as the best models a multiclass variant of LightGBM[20], a gradient boosting technique that uses tree-based learning, for the hand, and a fast implementation of Multiple Additive Regression Trees[21] for the feet, where LightGBM tends to overfit due to the smaller pixel dataset. The classifier was trained on the manually segmented hand and foot images and used to classify the pixels in the other hand and feet images.

3. RESULTS

Figures 3 and 4 are the reported representative multispectral image stacks of the hand and foot, particularly those used for training. In Figure 5 the training masks are presented, mapping the multispectral data on occluded (red), un-occluded (blue), background, and to-be-ignored areas (green). In Figure 6 a representative pixel classification on two hands (with and without occlusion) and on two feet (also with and without occlusion) is reported.

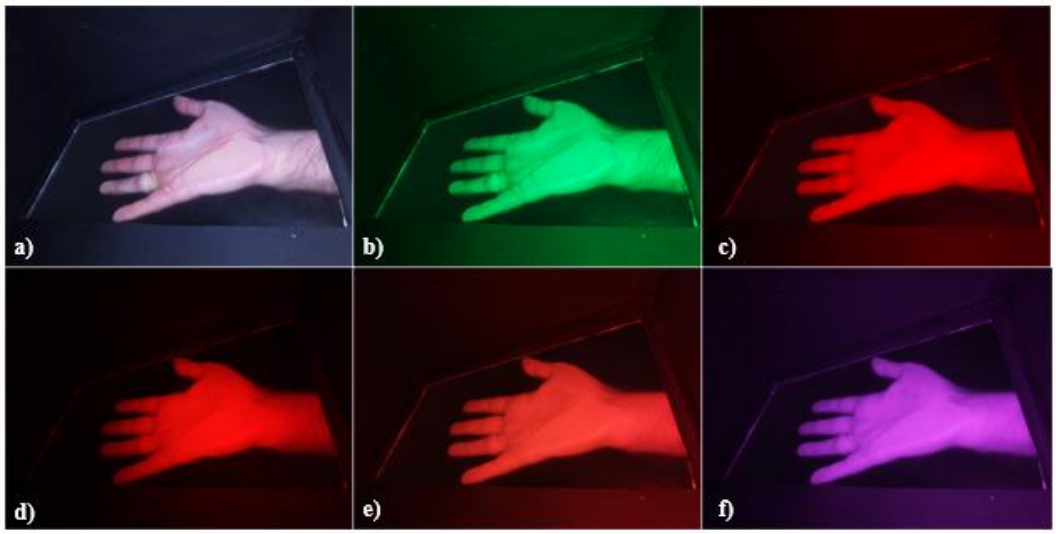

Figure 3. Reported representative multispectral image stacks of the hand with the MSI; a) White, b) Green, 525 nm c) Red, 633 nm d) 740 nm, e) 770 nm, f) 840 nm.

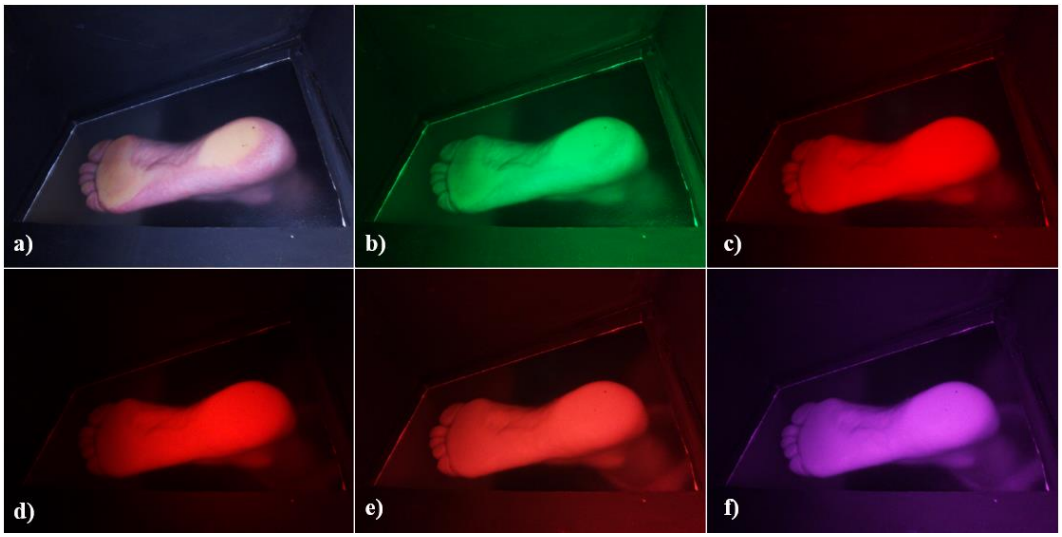

Figure 4. Reported representative multispectral image stacks of the hand with the MSI; a) White, b) Green, 525 nm c) Red, 633 nm d) 740 nm, e) 770 nm, f) 840 nm.

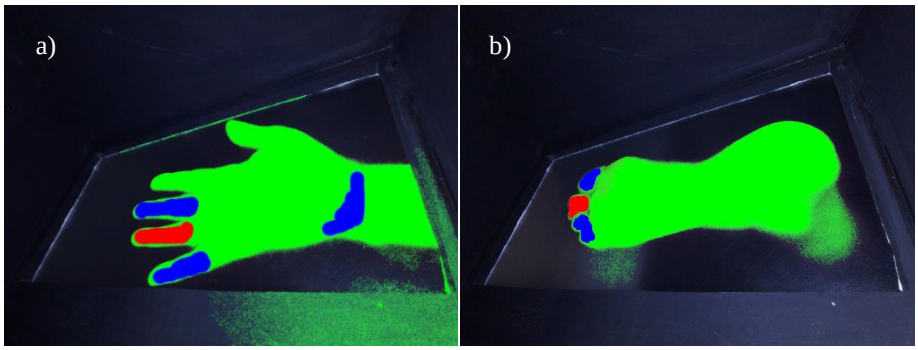

Figure 5. Training masks for the hand (a) and foot (b). The red pixels represent occluded areas, the blue pixels are non-occluded, and the green are pixels to be ignored during the training.

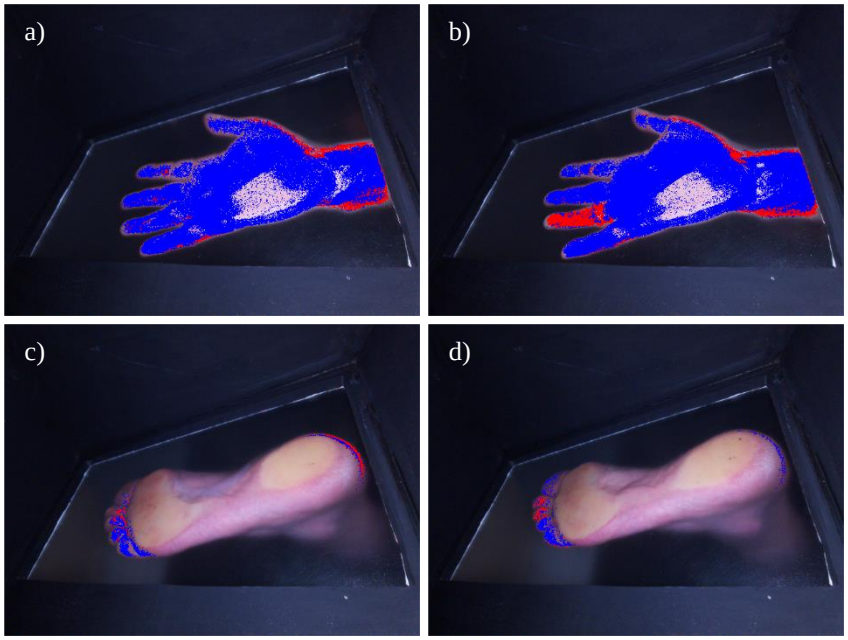

Figure 6. Pixel classification on the hand and foot, where red represents occluded and blue non-occluded pixels a) non-occluded hand, b) hand with one finger occluded, c) non-occluded foot, d) foot with two toes occluded.

4. DISCUSSION

Multispectral images have been successfully acquired on hands and feet. Even with the simplistic classification protocols used, the pixel classification, based on training on small areas of a single image, appears able to differentiate occluded vs non-occluded tissue, especially on the hands. Importantly, on the hand images, the training, performed on very small areas (the red and blue areas in Figure 5a) is sufficient to correctly classify most of the exposed skin (figures 5a and 5b). This gives some reassurance that the classification is being performed on the tissue spectra, rather than on simple channel intensity, which varies considerably across the hand surface. The same cannot be said for the feet images. We believe that, at this very preliminary stage, the number of pixels used for training of the foot classifier (red and blue areas on Figure 5b) is, essentially, insufficient. The AutoML library highlights this by converging onto a classifier requiring significantly less training data, and correctly identifying overfitting if using the same LightGBM classifier used for the hands. Also, occlusion of blood flow to a toe is difficult to achieve compared to a finger.

Indeed, these are very preliminary results. While the present work is mostly directed towards the description of the instrument, rather than of the data analytics, we note that these results, while indicative of the fact that the images contain the information we seek to extract, are still susceptible to significant improvement.

Firstly, the machine learning (ML) algorithm was trained, calibrated, and tested on a single subject which results in little variation within the dataset. This can cause biases that may not allow generalisation of the training. We note, however, that this device is designed for monitoring the progress of DFU, and therefore training on a single image of a single subject may well be acceptable for the intended use case, as this would in any case allow DFU progress monitoring. More importantly, the spectral data and related preprocessing used to train the ML algorithms is most likely redundant. Indeed, it is very likely that, albeit the different channels in the images carry independent information, correlations are high, and therefore the dataset would benefit from an initial dimensionality reduction.

Also importantly, we note significant variations in the intensity across the images. This points towards a sub-optimal illumination, also to be improved in the next iterations of the device. Indeed, the better classification of hand vs foot exposed areas might well be due to the smaller intensity variations across the hand surface with respect to the foot surface, ultimately ascribed to a better planarity of the hand with respect to the foot sole.

Finally, even though the device appears to be able to discriminate between perfused and under-perfused tissue already with the current simplistic data capture and analysis, little is known in the literature on whether this tissue differences are representative of early stages of DFU, and clinical trials should indeed be aimed to establishing whether this is the case.

ACKNOWLEDGEMENTS

This research was funded by the University of Strathclyde SRSS REA programme and IDCP Scotland Ltd.

REFERENCES

[1] "Global Report on Diabetes.", ISBN: 9789241565257, World Health Organisation (2016).
[2] McDermott, K., Fang, M., Boulton, A. J. M., Selvin, E. and Hicks, C. W., "Etiology, Epidemiology, and Disparities in the Burden of Diabetic Foot Ulcers," Diabetes Care 46(1), 209–221 (2022).
[3] "Diabetes and foot problems.", Diabetes UK, 18 July 2023, <https://www.diabetes.org.uk/guide-to-diabetes/complications/feet> (18 July 2023).
[4] Polikandrioti, M., Vasilopoulos, G., Koutelekos, I., Panoutsopoulos, G., Gerogianni, G., Babatsikou, F., Zartaloudi, A. and Toulia, G., "Quality of Life in Diabetic Foot Ulcer: Associated Factors and the Impact of Anxiety/Depression and Adherence to Self-Care," The International Journal of Lower Extremity Wounds 19(2), 165–179 (2020).
[5] "Diabetes & Foot Problems - NIDDK.", National Institute of Diabetes and Digestive and Kidney Diseases, <https://www.niddk.nih.gov/health-information/diabetes/overview/preventing-problems/foot-problems> (13 March 2024).
[6] Fard, A. S., Esmaelzadeh, M. and Larijani, B., "Assessment and treatment of diabetic foot ulcer," International Journal of Clinical Practice 61(11), 1779–1957 (2007).
[7] Monteiro-Soares, M., Vale-Lima, J., Martiniano, J., Pinheiro-Torres, S., Dias, V. and Boyko, E. J., "A systematic review with meta-analysis of the impact of access and quality of diabetic foot care delivery in preventing lower extremity amputation," Journal of Diabetes and its Complications 35(4), 107837 (2021).
[8] Crisologo, P. A. and Lavery, L. A., "Remote home monitoring to identify and prevent diabetic foot ulceration," 21, Annals of Translational Medicine 5(21), 430–430 (2017).
[9] Fayfman, M., Schechter, M. C., Amobi, C. N., Williams, R. N., Hillman, J. L., Alam, M. M., Rajani, R. R., Ziemer, D. C., Kempker, R. R. and Umpierrez, G. E., "Barriers to diabetic foot care in a disadvantaged population: A qualitative assessment," Journal of Diabetes and its Complications 34(12), 107688 (2020).
[10] Mullan, L., Driscoll, A., Wynter, K. and Rasmussen, B., "Barriers and enablers to delivering preventative and early intervention footcare to people with diabetes: a scoping review of healthcare professionals' perceptions," Aust. J. Prim. Health 25(6), 517–525 (2020).
[11] Bus, S. A., Stegge, W. B. aan de, Baal, J. G. van, Busch-Westbroek, T. E., Nollet, F. and Netten, J. J. van., "Effectiveness of at-home skin temperature monitoring in reducing the incidence of foot ulcer recurrence in people with diabetes: a multicenter randomized controlled trial (DIATEMP)," BMJ Open Diabetes Research and Care 9(1), e002392 (2021).
[12] "A home device for monitoring diabetic foot ulcers.", CORDIS | European Commission, 31 October 2019, <https://cordis.europa.eu/article/id/411457-a-home-device-for-monitoring-diabetic-foot-ulcers> (12 March 2024).
[13] Frykberg, R. G., Gordon, I. L., Reyzelman, A. M., Cazzell, S. M., Fitzgerald, R. H., Rothenberg, G. M., Bloom, J. D., Petersen, B. J., Linders, D. R., Nouvong, A. and Najafi, B., "Feasibility and Efficacy of a Smart Mat Technology to Predict Development of Diabetic Plantar Ulcers," Diabetes Care 40(7), 973–980 (2017).
[14] Willits, I., Cole, H., Jones, R., Dimmock, P., Arber, M., Craig, J. and Sims, A., "VibraTip™ for Testing Vibration Perception to Detect Diabetic Peripheral Neuropathy: A NICE Medical Technology Guidance," Appl Health Econ Health Policy 13(4), 315–324 (2015).
[15] Godavarty, A., Leiva, K., Amadi, N., Klonoff, D. C. and Armstrong, D. G., "Diabetic Foot Ulcer Imaging: An Overview and Future Directions," J Diabetes Sci Technol 17(6), 1662–1675 (2023).
[16] Basiri, A., Nabili, M., Mathews, S., Libin, A., Groah, S., Noordmans, H. J. and Ramella-Roman, J. C., "Use of a multi-spectral camera in the characterization of skin wounds," Opt. Express, OE 18(4), 3244–3257 (2010).

[17] Serena, T. E., Yaakov, R., Serena, L., Mayhugh, T. and Harrell, K., "Comparing near infrared spectroscopy and transcutaneous oxygen measurement in hard-to-heal wounds: a pilot study," J Wound Care 29(Sup6), S4–S9 (2020).
[18] Katsafadou, M. and Giardini, M. E., "Source multiplexing enhances the number of channels of a multispectral sensor," 2022 44th Annual International Conference of the IEEE Engineering in Medicine & Biology Society (EMBC), 2455–2458 (2022).
[19] "ML.NET | Machine learning made for .NET.", Microsoft, <https://dotnet.microsoft.com/en-us/apps/machinelearning-ai/ml-dotnet> (19 March 2024).
[20] "Welcome to LightGBM's documentation! — LightGBM 4.3.0.99 documentation.", <https://lightgbm.readthedocs.io/en/latest/index.html> (19 March 2024).
[21] "FastTreeBinaryTrainer Class (Microsoft.ML.Trainers.FastTree).", <https://learn.microsoft.com/en-us/dotnet/api/microsoft.ml.trainers.fasttree.fasttreebinarytrainer?view=ml-dotnet-2.0.0> (19 March 2024).